

Supporting Information

A carbon-oxygen-bridged hexacyclic ladder-type building block for low-bandgap nonfullerene acceptors

Ting Li,^{‡a,b} Honghong Zhang,^{‡b} Zuo Xiao,^b Jeromy J. Rech,^c Helin Niu,^{*a} Wei You^{*c} and Liming Ding^{*b}

a. School of Chemistry & Chemical Engineering, Anhui Province Key Laboratory of Chemistry for Inorganic/Organic Hybrid Functionalized Materials, Anhui University, Hefei 230601, China. E-mail: niuhelin@ahu.edu.cn

b. Center for Excellence in Nanoscience (CAS), Key Laboratory of Nanosystem and Hierarchical Fabrication (CAS), National Center for Nanoscience and Technology, Beijing 100190, China. E-mail: ding@nanoctr.cn

c. Department of Chemistry, University of North Carolina at Chapel Hill, NC 27599, USA. E-mail: wyou@unc.edu

[‡] T. Li and H. Zhang contributed equally to this work.

- 1. General characterization**
- 2. Synthesis**
- 3. NMR**
- 4. UV-Vis**
- 5. CV**
- 6. Device fabrication and measurements**
- 7. Optimization of device performance**
- 8. SCLC**
- 9. AFM**

1. General characterization

^1H and ^{13}C NMR spectra were measured on a Bruker Avance-400 spectrometer. Absorption spectra were recorded on a Shimadzu UV-1800 spectrophotometer. Cyclic voltammetry was done by using a Shanghai Chenhua CHI620D voltammetric analyzer under argon in an anhydrous acetonitrile solution of tetra-*n*-butylammonium hexafluorophosphate (0.1 M). A glassy-carbon electrode was used as the working electrode, a platinum-wire was used as the counter electrode, and a Ag/Ag⁺ electrode was used as the reference electrode. The donor or acceptor was coated onto glassy-carbon electrode and all potentials were corrected against Fc/Fc⁺. AFM was performed on a Multimode microscope (Veeco) using tapping mode.

2. Synthesis

All reagents were purchased from J&K Co., Aladdin Co., Innochem Co., Derthon Co., SunaTech Co. and other commercial suppliers. (3,6-dimethoxythieno[3,2-*b*]thiophene-2,5-diyl)bis(trimethylstannane),^[1] 2-ethylhexyl 2-bromothiophene-3-carboxylate^[2] and FTAZ^[3] were prepared according to literature.

Compound 1. To a solution of (3,6-dimethoxythieno[3,2-*b*]thiophene-2,5-diyl)bis(trimethylstannane) (526 mg, 1 mmol) and 2-ethylhexyl 2-bromothiophene-3-carboxylate (795 mg, 2.5 mmol) in toluene (30 mL) and DMF (3 mL) was added Pd(PPh₃)₄ (116 mg, 0.1 mmol) under argon. The mixture was heated to reflux for 48 h. After removal of the solvent, the crude product was purified via column chromatography (silica gel) by using CHCl₃ as eluent to give **compound 1** as a yellow oil (561 mg, 83%). ^1H NMR (CDCl₃, 400 MHz, δ /ppm): 7.50 (d, J = 5.4 Hz, 2H), 7.32 (d, J = 5.4 Hz, 2H), 4.08-4.23 (m, 4H), 3.97 (s, 6H), 1.53 (br, 2H), 1.13-1.40 (m, 16H), 0.72-0.97 (m, 12H). ^{13}C NMR (CDCl₃, 100 MHz, δ /ppm): 163.30, 147.81, 138.89, 131.27, 129.63, 127.93, 125.68, 114.03, 67.16, 59.31, 38.77, 30.32, 28.93, 23.64, 22.89, 14.06, 10.97. MALDI-TOF MS (m/z): 676.5 (M⁺).

Compound 2. To a solution of compound 1 (500 mg, 0.74 mmol) in dry CH₂Cl₂ (30 mL) was added BBr₃ (2.5 mL, 1.75 M, 4.44 mmol) at room temperature under argon. The mixture was stirred for 2.5 h and was quenched by adding H₂O (3 mL). The organic layer was directly submitted to a silica gel column with CHCl₃ as the eluent. **Compound 2** was obtained as a yellow solid (455 mg, 95%). ^1H NMR (DMSO-*d*₆, 400 MHz, δ /ppm): 10.46 (s, 2H), 7.62 (d, J

= 5.4 Hz, 2H), 7.40 (d, J = 5.4 Hz, 2H), 4.04 (d, J = 5.4 Hz, 4H), 1.46 (br, 2H), 1.13-1.22 (m, 16H), 0.61-0.91 (m, 12H). ^{13}C NMR (DMSO- d_6 , 100 MHz, δ /ppm): 163.12, 145.22, 139.52, 129.89, 129.19, 127.48, 126.34, 108.62, 66.41, 38.89, 29.82, 28.44, 23.10, 22.34, 13.97, 10.83. MALDI-TOF MS (m/z): 671.5 ($M + \text{Na}^+$).

Compound 3. To a solution of compound 2 (455 mg, 0.7 mmol) in toluene (20 mL) was added *p*-toluenesulfonic acid (120 mg, 0.7 mmol) at room temperature. The mixture was stirred at 110 °C for 1 h and was poured into MeOH. The precipitate was collected and dried under vacuum to give **compound 3** as a yellow solid (272 mg, 100%). NMR data were not acquired due to the extremely low solubility of compound 3.

CO₆. To compound 3 (272 mg, 0.7 mmol) was added (4-hexylphenyl)magnesium bromide (7 mL, 1 M in THF, 7 mmol) at room temperature under argon. The mixture was stirred at 60 °C for 12 h. After cooling to room temperature, the reaction mixture was poured into ice water followed by extraction with CH_2Cl_2 three times. The combined organic layer was dried over anhydrous Na_2SO_4 . After removal of the solvent, the residue was dissolved in toluene (20 mL) and *p*-toluenesulfonic acid (240 mg, 1.4 mmol) was added. The mixture was stirred at room temperature for 1 h and was poured into MeOH. The precipitate was collected and purified via column chromatography (silica gel) by using CHCl_3 as eluent to give **CO₆** as a yellow solid (603 mg, 86%). ^1H NMR (CDCl_3 , 400 MHz, δ /ppm): 7.17 (d, J = 8.1 Hz, 8H), 7.09 (d, J = 8.1 Hz, 8H), 7.02 (d, J = 5.0 Hz, 2H), 6.46 (d, J = 5.0 Hz, 2H), 2.56 (t, J = 7.7 Hz, 2H), 1.52-1.64 (m, 12H), 1.29 (s, 24H), 0.85-0.87 (m, 12H). ^{13}C NMR (CDCl_3 , 100 MHz, δ /ppm): 143.30, 142.78, 140.75, 133.03, 129.92, 127.82, 127.80, 127.63, 125.25, 120.49, 113.57, 88.65, 35.61, 31.68, 31.20, 29.10, 22.57, 14.07. MALDI-TOF MS (m/z): 1001.9 ($M + \text{H}^+$).

CO₆-CHO. To a solution of CO₆ (600 mg, 0.6 mmol) in dry THF (100 mL) was added *n*-BuLi (1.13 mL, 1.6 M, 1.8 mmol) at -78 °C under argon. The resulting mixture was warmed to -50 °C and stirred for 1.5 h. To the mixture was added *N,N*-dimethylformamide (475 μL , 6 mmol). The resulting mixture was stirred for 1 h and was then quenched by water followed by extraction with CH_2Cl_2 three times. The combined organic layer was dried over anhydrous Na_2SO_4 . After removal of the solvent, the crude product was purified via column chromatography (silica gel) by using CH_2Cl_2 :petroleum ether (1:2) as eluent to give **CO₆-CHO** as an orange solid (507 mg, 80%). ^1H NMR (CDCl_3 , 400 MHz, δ /ppm): 9.72 (s, 2H),

7.14 (m, 16H), 7.08 (s, 2H), 2.54-2.64 (m, 8H), 1.54-1.66 (m, 8H), 1.24-1.37 (m, 24H), 0.87 (t, $J = 6.6$ Hz, 12H). ^{13}C NMR (CDCl_3 , 100 MHz, δ/ppm): 181.81, 146.27, 143.57, 139.45, 139.26, 138.79, 136.21, 134.06, 128.17, 127.69, 127.52, 114.79, 88.71, 35.60, 31.66, 31.17, 29.07, 22.56, 14.06. MALDI-TOF MS (m/z): 1058.0 ($\text{M} + \text{H}^+$).

CO₆IC. To a solution of CO₆-CHO (100 mg, 0.095 mmol) in CHCl_3 (15 mL) was added 2-(3-oxo-2,3-dihydro-1H-inden-1-ylidene)malononitrile (IC) (114 mg, 0.95 mmol) and pyridine (0.3 mL) at room temperature. The mixture was heated to reflux for 12 h. After removal of the solvent, the crude product was purified via column chromatography (silica gel) by using CHCl_3 as eluent to give **CO₆IC** as a black solid (120 mg, 90%). ^1H NMR (THF-d_8 , 400 MHz, δ/ppm): 8.62 (s, 2H), 8.14 (d, $J = 6.8$ Hz, 2H), 7.76-7.85 (m, 4H), 7.62-7.74 (m, 4H), 7.20 (m, 16H), 2.54-2.70 (m, 8H), 1.59-1.63 (m, 8H), 1.30-1.36 (m, 24H), 0.87 (t, $J = 6.8$ Hz, 12H). ^{13}C NMR (CDCl_3 , 100 MHz, δ/ppm): 188.06, 159.27, 147.52, 144.50, 139.74, 139.41, 136.61, 136.45, 134.87, 134.57, 128.68, 128.28, 124.70, 123.33, 114.73, 114.59, 67.82, 35.66, 31.67, 31.11, 29.23, 22.61, 14.08. MALDI-TOF MS (m/z): 1409.6 (M^+).

CO₆FIC. To a solution of CO₆-CHO (70 mg, 0.066 mmol) in CHCl_3 (20 mL) was added FIC (two isomers) (70 mg, 0.33 mmol) and pyridine (0.5 mL) at room temperature. The mixture was heated to reflux for 12 h. After removal of the solvent, the crude product was purified via column chromatography (silica gel) by using CHCl_3 as eluent to give **CO₆FIC** as a black solid (90 mg, 94%). ^1H NMR (THF-d_8 , 400 MHz, δ/ppm): 8.68 (m, 2H), 8.23 (br), 7.86 (br), 7.20-7.64 (br), 2.60 (m, 8H), 1.60 (m, 8H), 1.31 (m, 24H), 0.87 (m, 12H). ^{13}C NMR (CDCl_3 , 100 MHz, δ/ppm): 186.71, 167.79, 165.22, 157.90, 147.81, 147.77, 147.66, 144.81, 143.92, 141.86, 141.76, 139.50, 136.81, 136.64, 135.29, 135.00, 134.17, 132.64, 128.87, 128.30, 125.55, 125.45, 121.95, 121.73, 119.99, 117.02, 114.47, 114.39, 114.06, 112.48, 112.22, 89.17, 68.55, 67.71, 35.65, 31.68, 31.09, 29.21, 22.61, 14.08. MALDI-TOF MS (m/z): 1446.8 ($\text{M} + \text{H}^+$).

CO₆DFIC. To a solution of CO₆-CHO (70 mg, 0.066 mmol) in CHCl_3 (20 mL) was added DFIC (76 mg, 0.33 mmol) and pyridine (0.5 mL) at room temperature. The mixture was heated to reflux for 12 h. After removal of the solvent, the crude product was purified via column chromatography (silica gel) by using CHCl_3 as eluent to give **CO₆DFIC** as a black solid (84 mg, 86%). ^1H NMR (THF-d_8 , 400 MHz, δ/ppm): 8.60 (s, 2H), 8.11 (br, 2H), 7.78 (m, 2H), 7.19-7.36 (br, 18H), 2.60 (m, 8H), 1.61 (m, 8H), 1.30-1.36 (m, 24H), 0.87 (m, 12H). ^{13}C

NMR (CDCl₃, 100 MHz, δ /ppm): 185.82, 157.11, 148.02, 147.91, 145.15, 144.04, 139.31, 136.69, 135.33, 134.07, 129.07, 128.34, 128.05, 119.36, 117.15, 114.69, 114.48, 114.07, 113.99, 112.49, 112.30, 89.24, 68.47, 35.64, 31.67, 31.07, 29.19, 26.90, 22.60, 14.07.
MALDI-TOF MS (m/z): 1482.7 (M + H⁺).

3. NMR

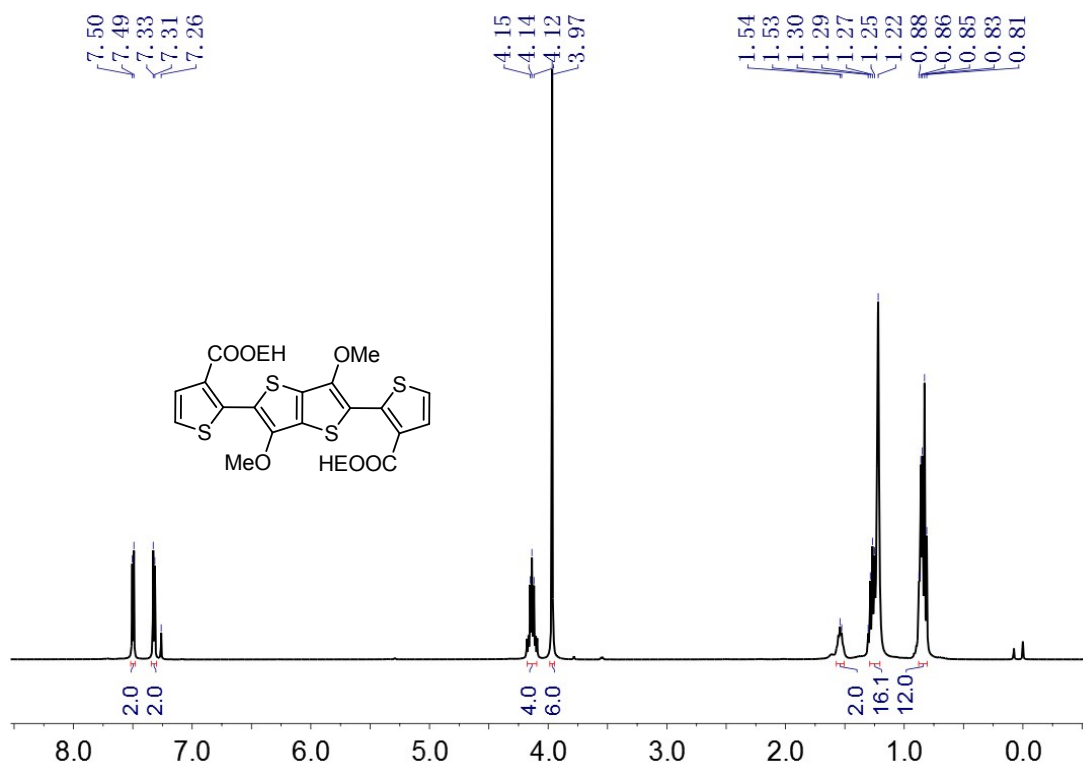


Fig. S1 ^1H NMR spectrum of Compound 1.

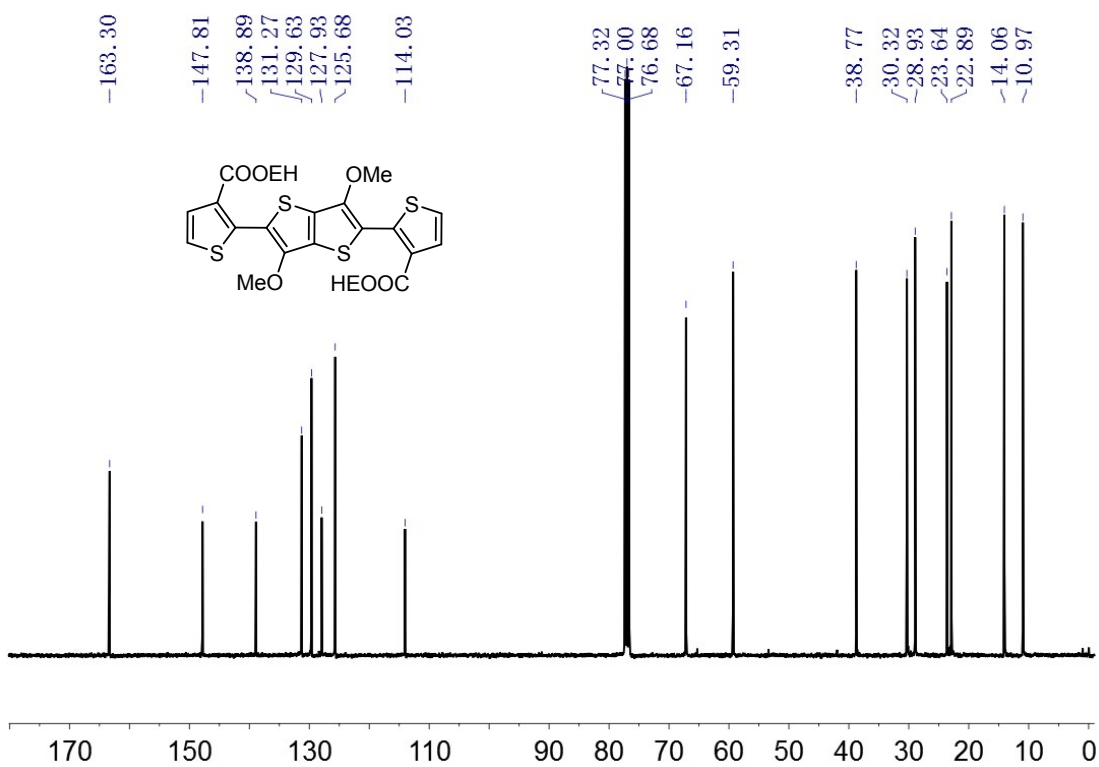


Fig. S2 ^{13}C NMR spectrum of Compound 1.

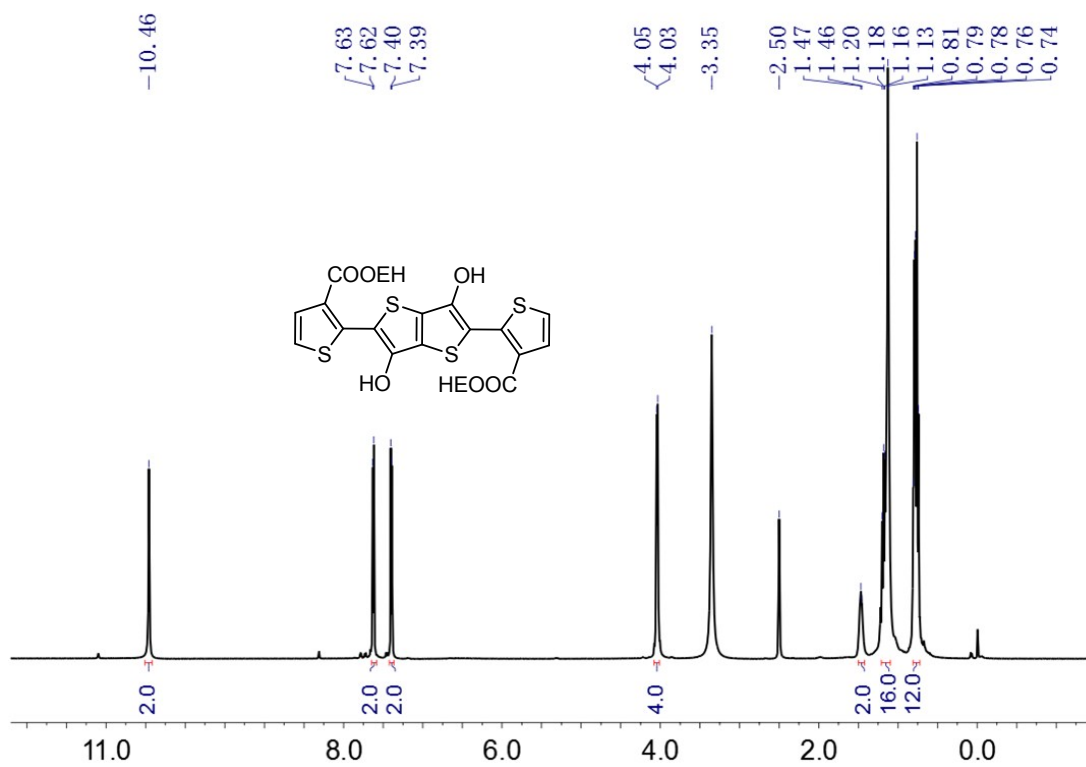


Fig. S3 ^1H NMR spectrum of Compound 2.

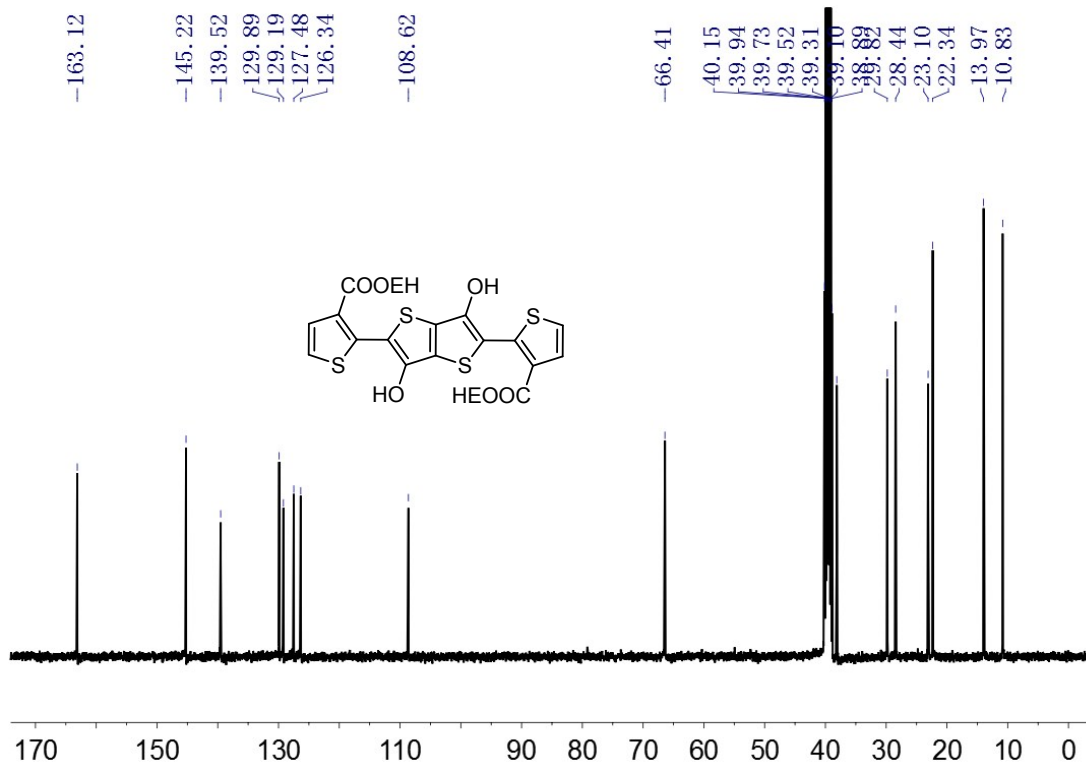


Fig. S4 ^{13}C NMR spectrum of Compound 2.

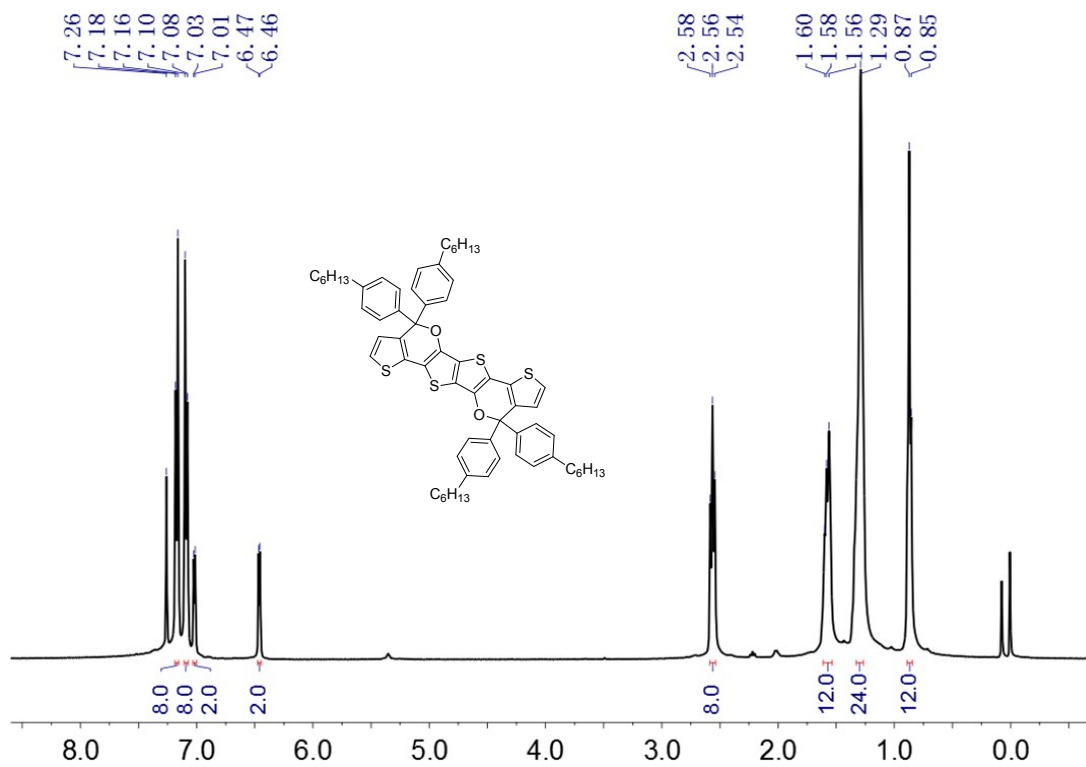


Fig. S5 ^1H NMR spectrum of $\text{CO},6$.

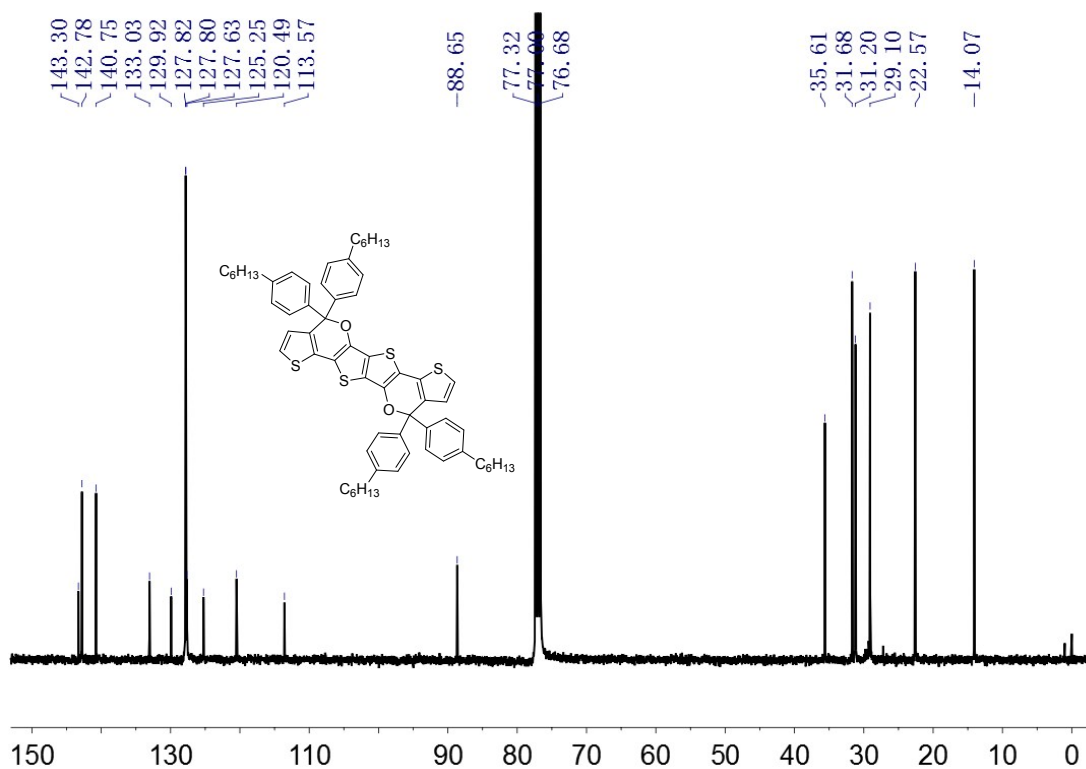


Fig. S6 ^{13}C NMR spectrum of $\text{CO},6$.

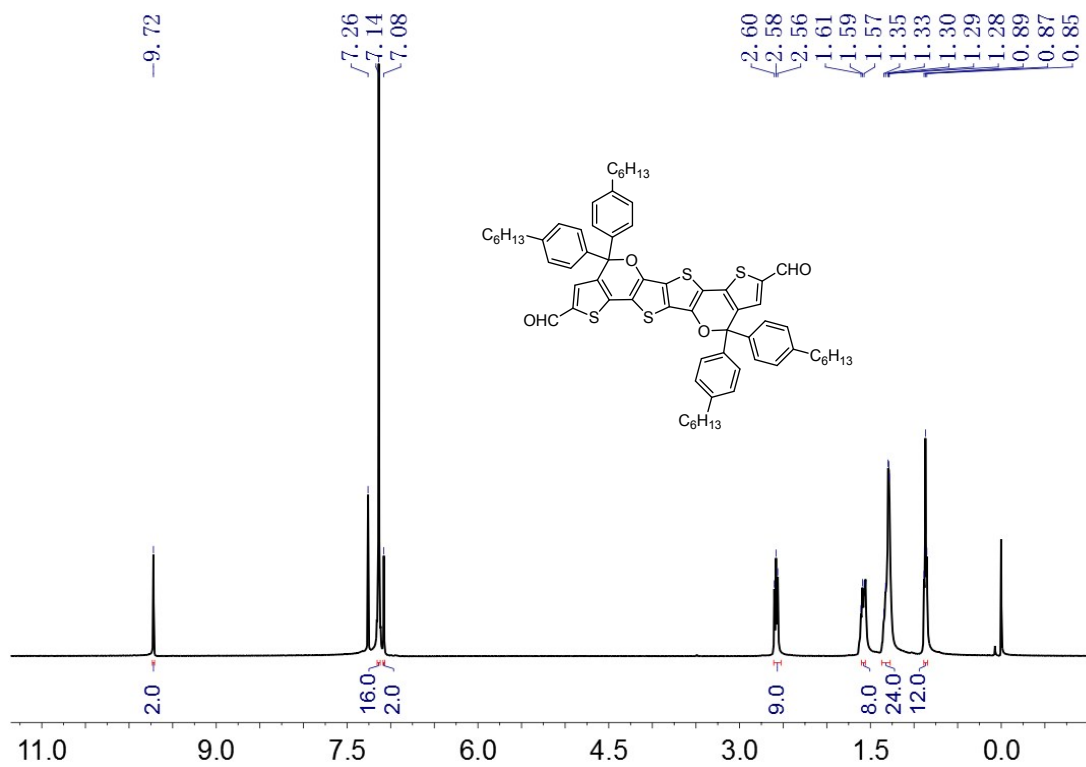


Fig. S7 ^1H NMR spectrum of $\text{CO}_6\text{-CHO}$.

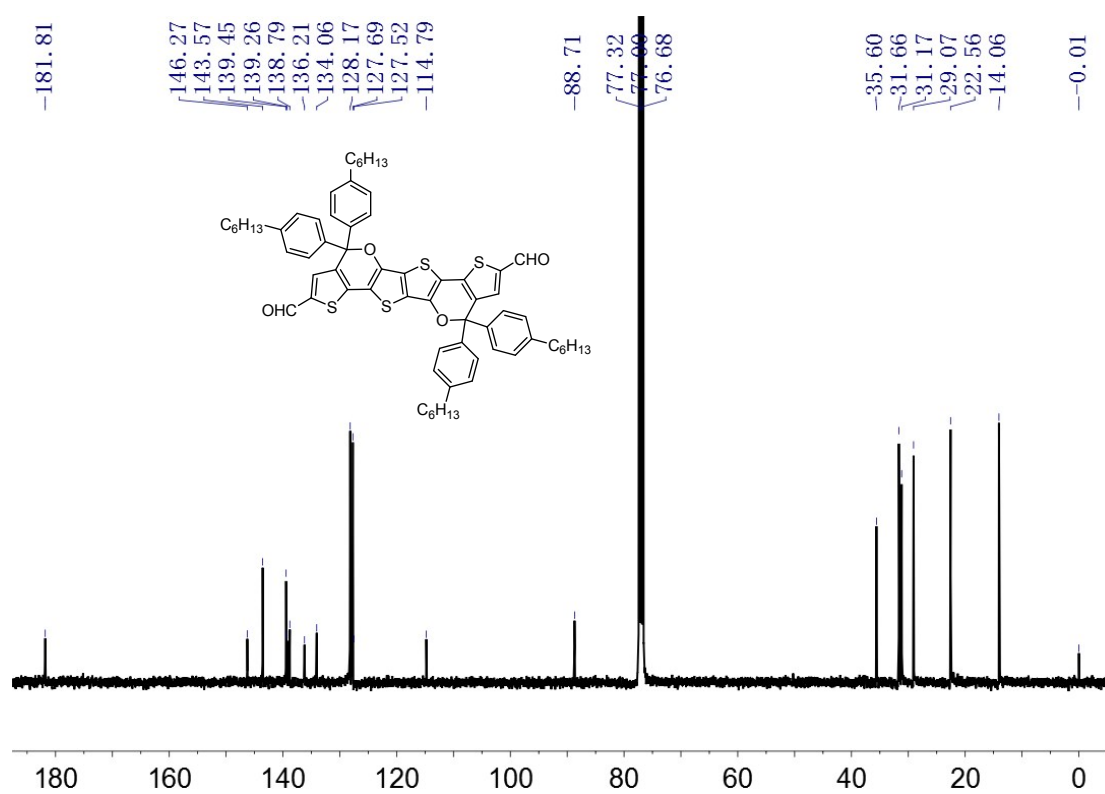


Fig. S8 ^{13}C NMR spectrum of $\text{CO}_6\text{-CHO}$.

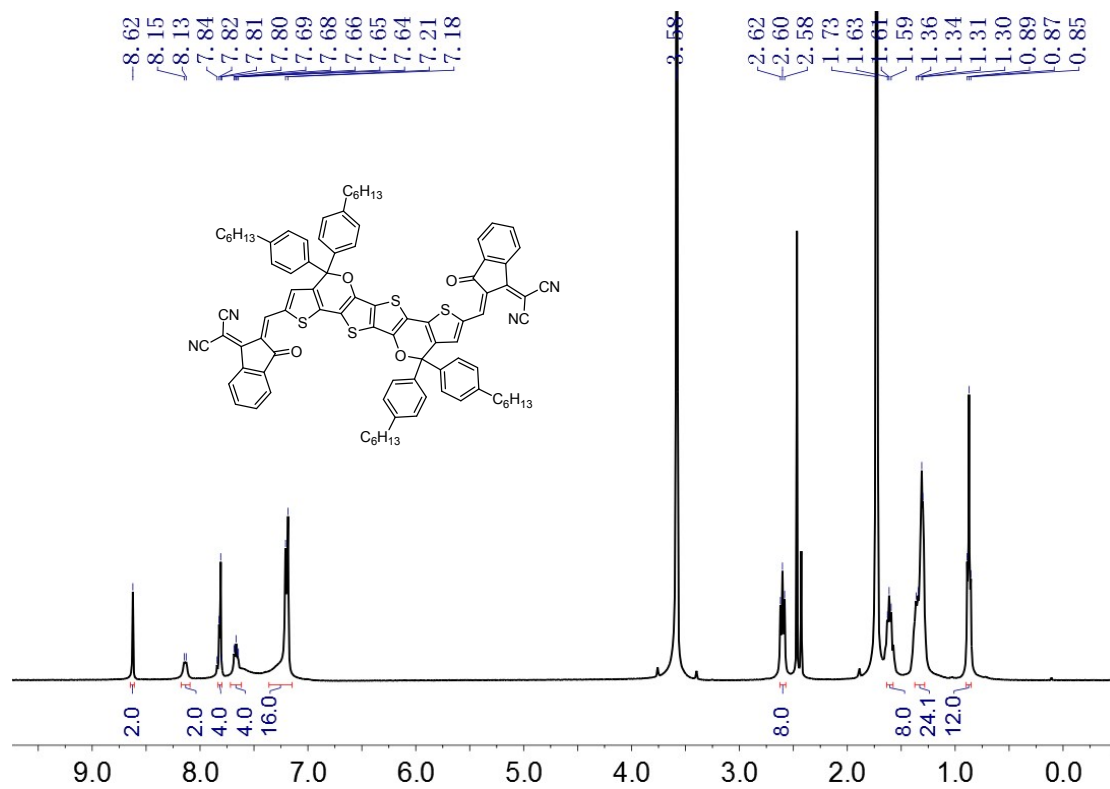


Fig. S9 ¹H NMR spectrum of CO₆IC.

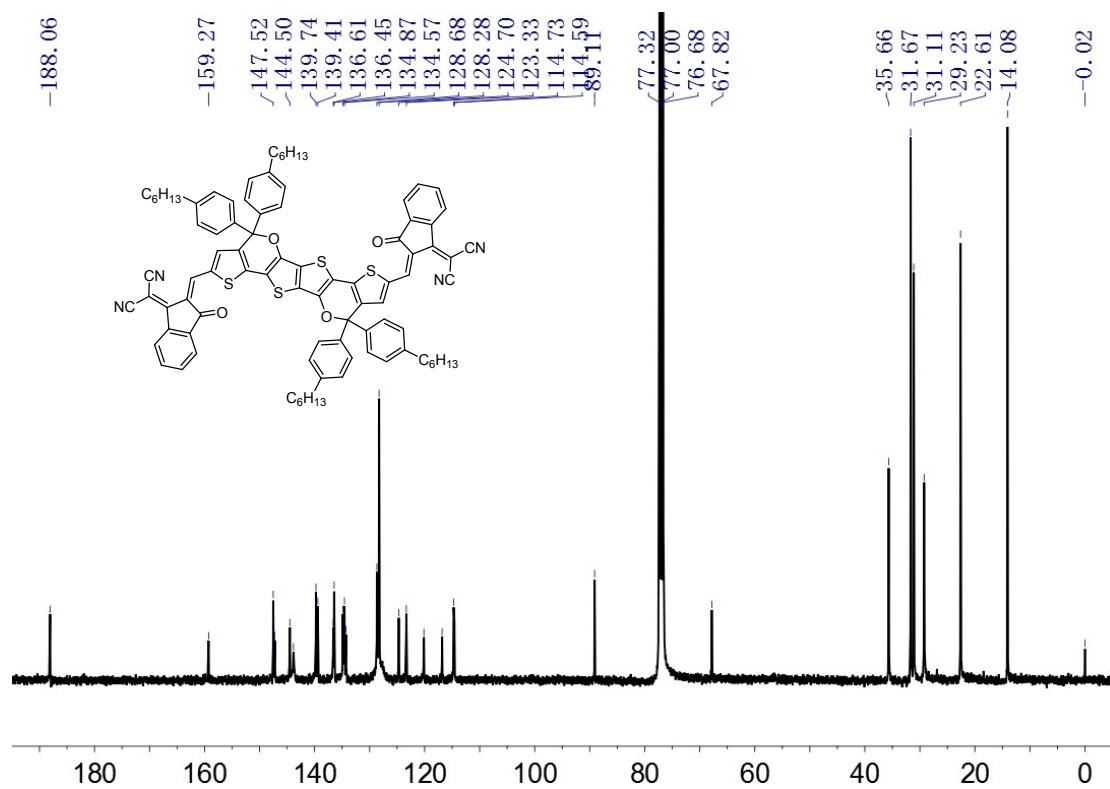


Fig. S10 ¹³C NMR spectrum of CO₆IC.

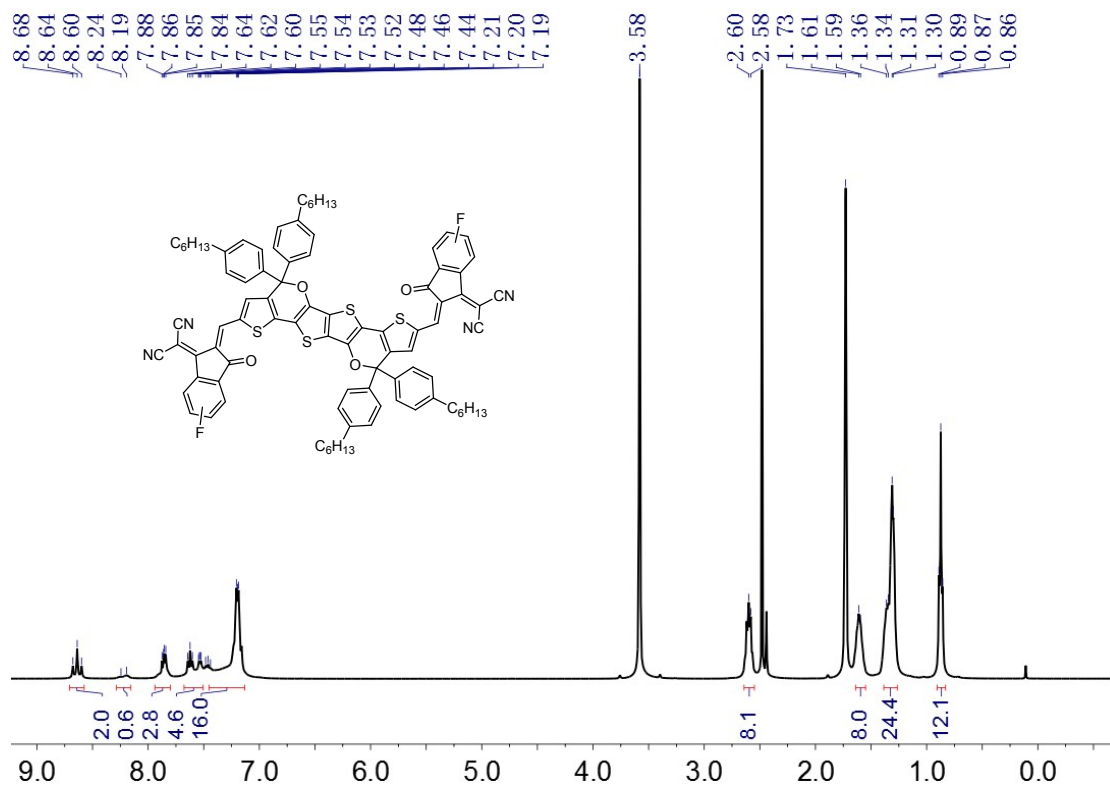


Fig. S11 ^1H NMR spectrum of $\text{CO}_7\text{6FIC}$.

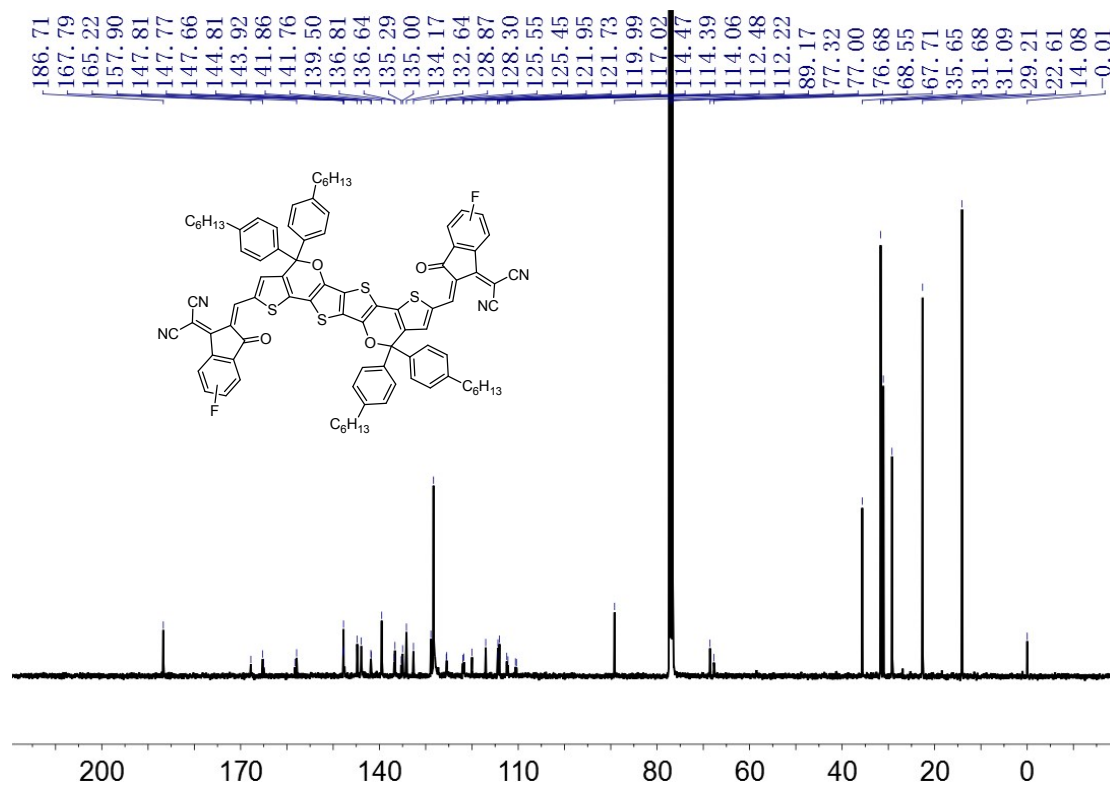


Fig. S12 ^{13}C NMR spectrum of $\text{CO}_7\text{6FIC}$.

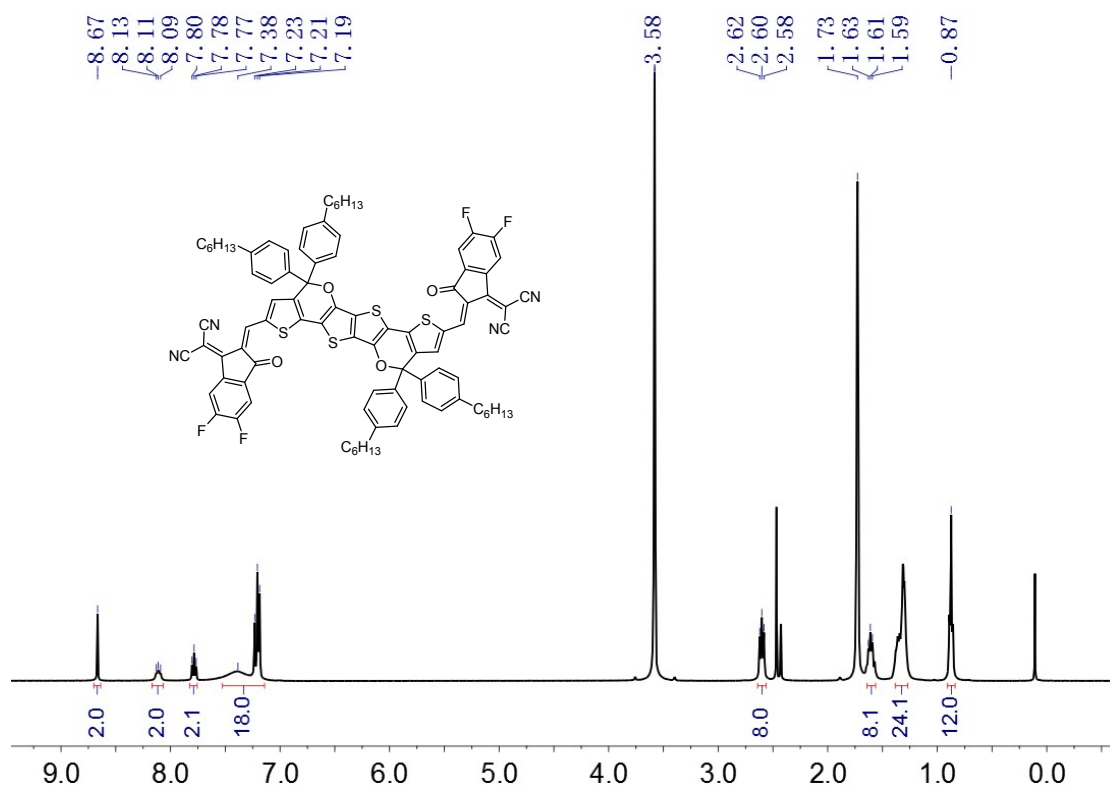


Fig. S13 ¹H NMR spectrum of CO₆DFIC.

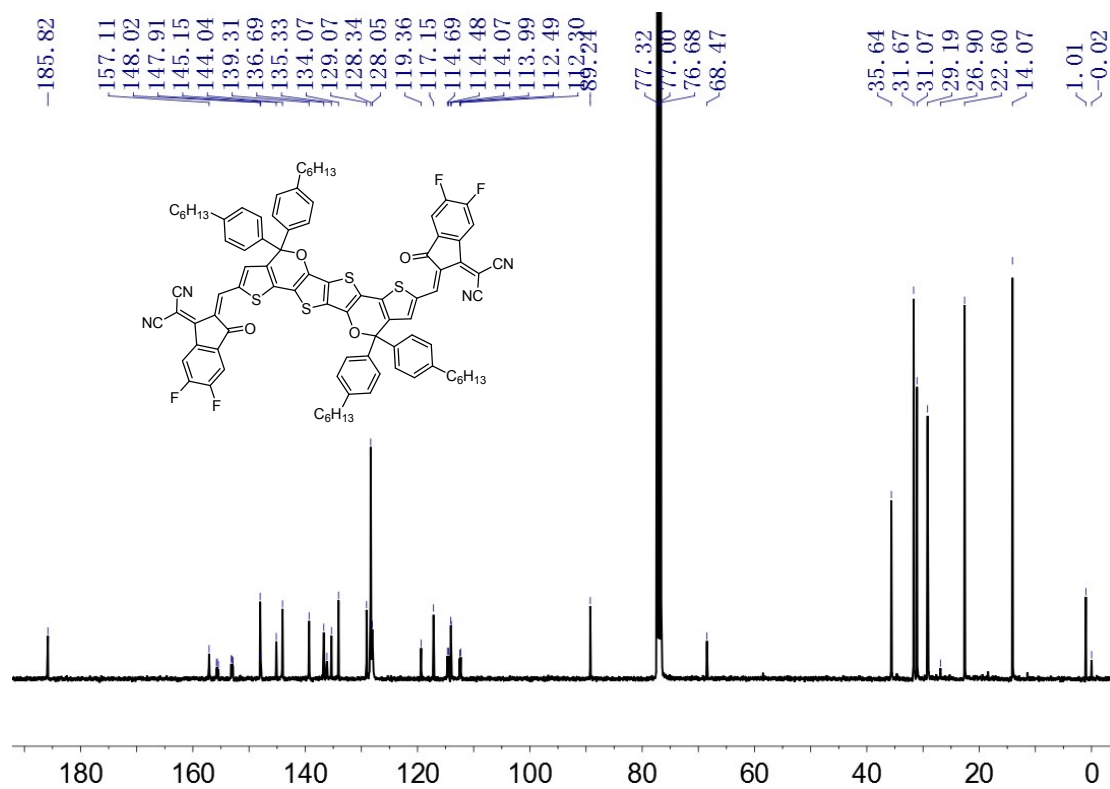


Fig. S14 ¹³C NMR spectrum of CO₆DFIC.

4. UV-Vis

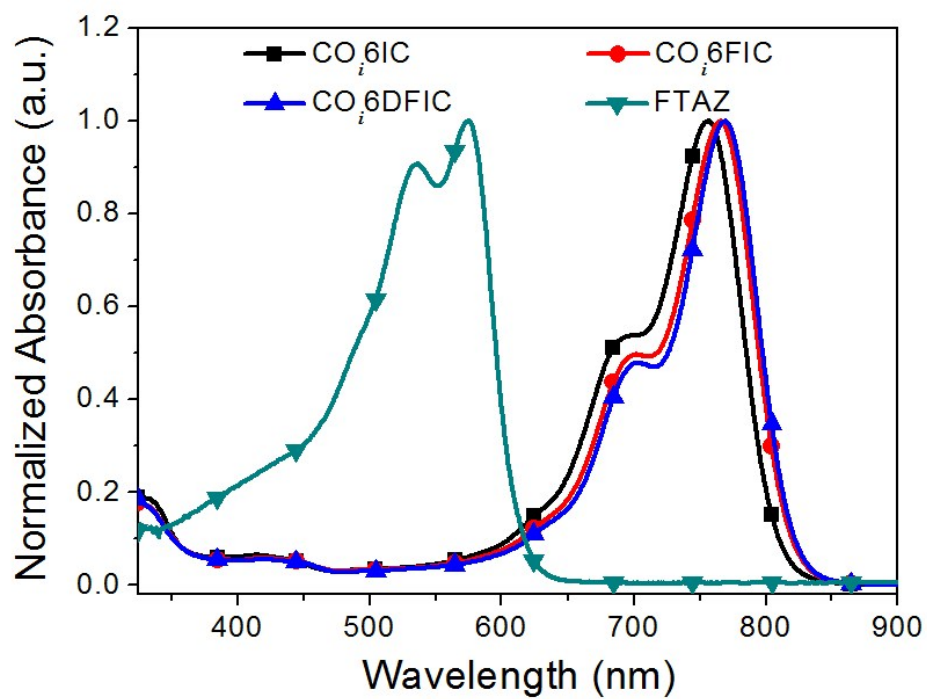


Fig S15. Absorption spectra for CO_i6IC, CO_i6FIC, CO_i6DFIC and FTAZ in solution.

5. CV

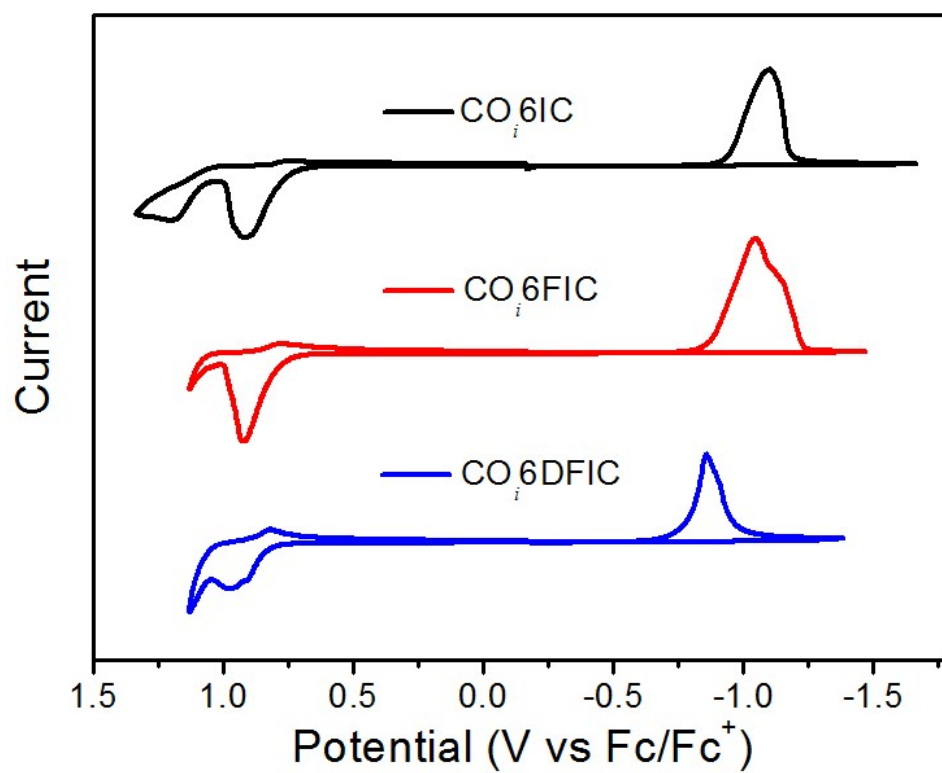


Fig. S16 Cyclic voltammograms for CO₆IC, CO₆FIC and CO₆DFIC.

6. Device fabrication and measurements

Inverted solar cells

The ZnO precursor solution was prepared according to literature.^[4] It was spin-coated onto ITO glass (4000 rpm for 30 s). The films were annealed at 200 °C in air for 30 min. ZnO film thickness is ~30 nm. A FTAZ:acceptor blend in chloroform (CF) with DIO additive was spin-coated onto ZnO layer. MoO₃ (~6 nm) and Ag (~80 nm) was successively evaporated onto the active layer through a shadow mask (pressure ca. 10⁻⁴ Pa). The effective area for the devices is 4 mm². The thicknesses of the active layers were measured by using a KLA Tencor D-120 profilometer. *J-V* curves were measured by using a computerized Keithley 2400 SourceMeter and a Xenon-lamp-based solar simulator (Enli Tech, AM 1.5G, 100 mW/cm²). The illumination intensity of solar simulator was determined by using a monocrystalline silicon solar cell (Enli SRC2020, 2cm×2cm) calibrated by NIM. The external quantum efficiency (EQE) spectra were measured by using a QE-R3011 measurement system (Enli Tech).

Hole-only devices

The structure for hole-only devices is ITO/PEDOT:PSS/FTAZ:acceptor/MoO₃/Al. A 30 nm thick PEDOT:PSS layer was made by spin-coating an aqueous dispersion onto ITO glass (4000 rpm for 30 s). PEDOT substrates were dried at 150 °C for 10 min. A FTAZ:acceptor blend in CF with DIO additive was spin-coated onto PEDOT layer. Finally, MoO₃ (~6 nm) and Al (~100 nm) was successively evaporated onto the active layer through a shadow mask (pressure ca. 10⁻⁴ Pa). *J-V* curves were measured by using a computerized Keithley 2400 SourceMeter in the dark.

Electron-only devices

The structure for electron-only devices is Al/FTAZ:acceptor/Ca/Al. Al (~80 nm) was evaporated onto a glass substrate. A FTAZ:acceptor blend in CF with DIO additive was spin-coated onto Al. Ca (~5 nm) and Al (~100 nm) were successively evaporated onto the active layer through a shadow mask (pressure ca. 10⁻⁴ Pa). *J-V* curves were measured by using a computerized Keithley 2400 SourceMeter in the dark.

7. Optimization of device performance

Table S1 Optimization of D/A ratio for FTAZ:CO₆IC inverted solar cells.^a

D/A [w/w]	V_{oc} [V]	J_{sc} [mA/cm ²]	FF [%]	PCE [%]
1:1	0.82	14.60	45.8	5.52 (5.34) ^b
1:1.2	0.83	14.87	49.0	6.07 (5.82)
1:1.4	0.82	15.43	51.1	6.50 (6.35)
1:1.6	0.82	15.75	55.2	7.10 (6.94)
1:1.8	0.83	15.74	52.7	6.88 (6.68)
1:2	0.83	15.10	51.5	6.46 (6.21)

^aBlend solution: 12 mg/mL in CF; spin-coating: 4000 rpm for 30 s.

^bData in parentheses stand for the average PCEs for 8 cells.

Table S2 Optimization of the active layer thickness for FTAZ:CO₆IC inverted solar cells.^a

Thickness [nm]	V_{oc} [V]	J_{sc} [mA/cm ²]	FF [%]	PCE [%]
98	0.82	15.53	52.2	6.61 (6.40) ^b
85	0.82	15.75	55.2	7.10 (6.94)
80	0.82	15.46	53.4	6.74 (6.50)
73	0.81	15.05	50.2	6.14 (5.93)

^aD/A ratio: 1:1.6 (w/w); blend solution: 12 mg/mL in CF.

^bData in parentheses stand for the average PCEs for 8 cells.

Table S3 Optimization of DIO content for FTAZ:CO₆IC inverted solar cells.^a

DIO [vol%]	V_{oc} [V]	J_{sc} [mA/cm ²]	FF [%]	PCE [%]
0	0.82	15.75	55.2	7.10 (6.79) ^b
0.1	0.82	17.20	57.6	8.21 (8.03)
0.2	0.82	17.45	59.0	8.43 (8.35)
0.3	0.82	16.91	53.2	7.45 (7.29)

^aD/A ratio: 1:1.6 (w/w); blend solution: 12 mg/mL in CF; spin-coating: 4000 rpm for 30 s.

^bData in parentheses stand for the average PCEs for 8 cells.

Table S4 Optimization of D/A ratio for FTAZ:CO₆FIC inverted solar cells.^a

D/A [w/w]	V_{oc} [V]	J_{sc} [mA/cm ²]	FF [%]	PCE [%]
1:1	0.75	17.69	52.3	6.91 (6.70) ^b
1:1.2	0.74	18.27	53.9	7.25 (6.98)
1:1.4	0.74	18.38	57.9	7.85 (7.61)
1:1.6	0.75	18.63	58.5	8.13 (7.89)
1:1.8	0.73	18.30	56.1	7.54 (7.30)
1:2	0.74	17.82	54.5	7.15 (6.80)

^aBlend solution: 12 mg/mL in CF; spin-coating: 4000 rpm for 30 s.

^bData in parentheses stand for the average PCEs for 8 cells.

Table S5 Optimization of the active layer thickness for FTAZ:CO₆FIC inverted solar cells.^a

Thickness [nm]	V_{oc} [V]	J_{sc} [mA/cm ²]	FF [%]	PCE [%]
95	0.75	18.09	53.1	7.24 (6.95) ^b
87	0.75	18.63	58.5	8.13 (7.89)
80	0.74	18.54	54.6	7.47 (7.20)
76	0.74	18.14	54.5	7.27 (7.03)

^aD/A ratio: 1:1.6 (w/w); blend solution: 12 mg/mL in CF.

^bData in parentheses stand for the average PCEs for 8 cells.

Table S6 Optimization of DIO content for FTAZ:CO₆FIC inverted solar cells.^a

DIO [vol%]	V_{oc} [V]	J_{sc} [mA/cm ²]	FF [%]	PCE [%]
0	0.75	18.63	58.5	8.13 (7.89) ^b
0.1	0.74	19.31	60.9	8.71 (8.50)
0.2	0.75	19.38	62.6	9.12 (9.02)
0.3	0.74	18.95	58.1	8.17 (8.04)

^aD/A ratio: 1:1.6 (w/w); blend solution: 12 mg/mL in CF; spin-coating: 4000 rpm for 30 s.

^bData in parentheses stand for the average PCEs for 8 cells.

Table S7 Optimization of D/A ratio for FTAZ:CO₆DFIC inverted solar cells.^a

D/A	V_{oc}	J_{sc}	FF	PCE
[w/w]	[V]	[mA/cm ²]	[%]	[%]
1:1	0.68	15.46	48.9	5.16 (4.91) ^b
1:1.2	0.68	17.01	49.5	5.73 (5.54)
1:1.4	0.68	17.22	50.7	5.96 (5.71)
1:1.6	0.68	18.27	51.7	6.36 (6.15)
1:1.8	0.68	17.15	51.2	6.02 (5.85)
1:2	0.68	16.61	51.9	5.87 (5.60)

^aBlend solution: 12 mg/mL in CF; spin-coating: 4000 rpm for 30 s.

^bData in parentheses stand for the average PCEs for 8 cells.

Table S8 Optimization of the active layer thickness for FTAZ:CO₆DFIC inverted solar cells.^a

Thickness	V_{oc}	J_{sc}	FF	PCE
[nm]	[V]	[mA/cm ²]	[%]	[%]
91	0.68	17.60	48.3	5.75 (5.53) ^b
83	0.68	18.27	51.7	6.36 (6.15)
75	0.68	17.40	50.0	5.94 (5.76)
69	0.68	16.70	48.4	5.52 (5.32)

^aD/A ratio: 1:1.6 (w/w); blend solution: 12 mg/mL in CF.

^bData in parentheses stand for the average PCEs for 8 cells.

Table S9 Optimization of DIO content for FTAZ:CO₆DFIC inverted solar cells.^a

DIO [vol%]	V_{oc} [V]	J_{sc} [mA/cm ²]	FF [%]	PCE [%]
0	0.68	18.27	51.7	6.36 (6.15) ^b
0.1	0.66	20.70	55.8	7.63 (7.35)
0.2	0.67	20.98	58.9	8.25 (8.11)
0.3	0.66	20.12	56.0	7.42 (7.19)

^aD/A ratio: 1:1.6 (w/w); blend solution: 12 mg/mL in CF; spin-coating: 4000 rpm for 30 s.

^bData in parentheses stand for the average PCEs for 8 cells.

8. SCLC

Charge carrier mobility was measured by SCLC method. The mobility was determined by fitting the dark current to the model of a single carrier SCLC, which is described by:

$$J = \frac{9}{8} \varepsilon_0 \varepsilon_r \mu \frac{V^2}{d^3}$$

where J is the current density, μ is the zero-field mobility of holes (μ_h) or electrons (μ_e), ε_0 is the permittivity of the vacuum, ε_r is the relative permittivity of the material, d is the thickness of the blend film, and V is the effective voltage ($V = V_{\text{appl}} - V_{\text{bi}}$, where V_{appl} is the applied voltage, and V_{bi} is the built-in potential determined by electrode work function difference). Here, $V_{\text{bi}} = 0.1$ V for hole-only devices, $V_{\text{bi}} = 0$ V for electron-only devices.^[5] The mobility was calculated from the slope of $J^{1/2}$ - V plots.

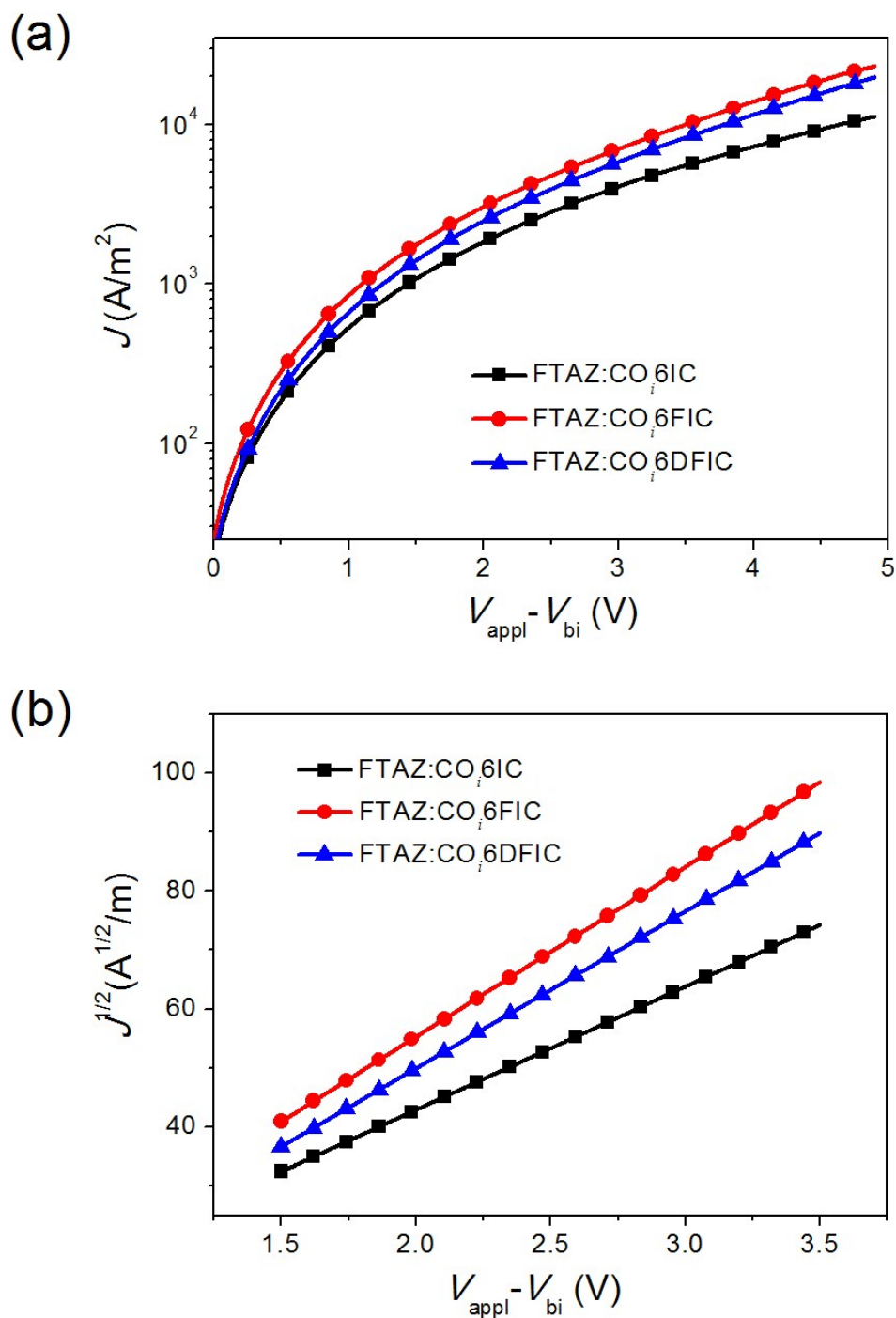


Fig. S17 J - V curves (a) and corresponding $J^{1/2}$ - V plots (b) for the hole-only devices (in dark). The thicknesses for FTAZ:CO₆IC, FTAZ:CO₆FIC and FTAZ:CO₆DFIC blend films with 0.2 vol% DIO are 83, 85 and 79 nm, respectively.

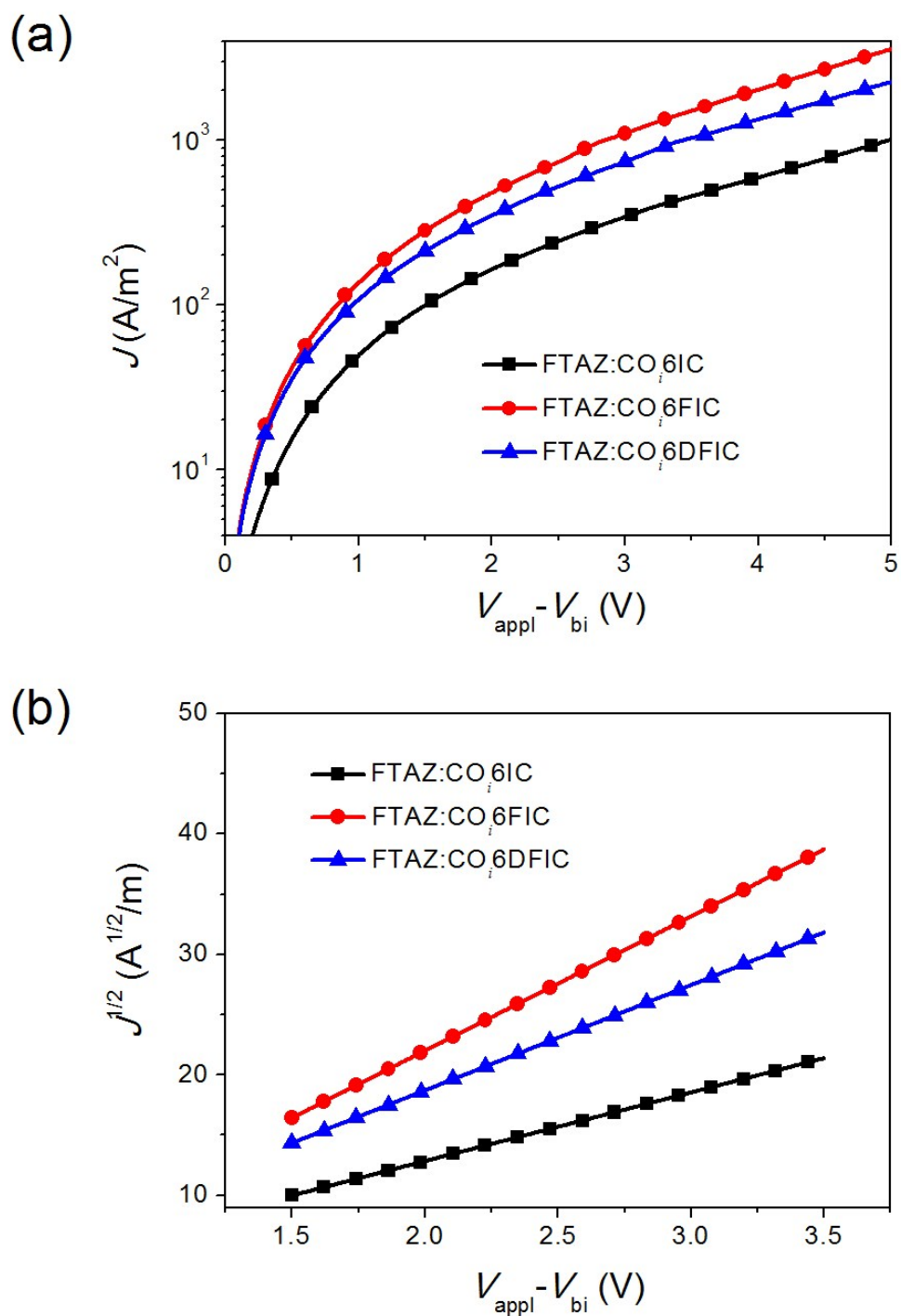


Fig. S18 J - V curves (a) and corresponding $J^{1/2}$ - V plots (b) for the electron-only devices (in dark). The thicknesses for FTAZ:CO₆I₆C, FTAZ:CO₆F₆C and FTAZ:CO₆D₆F₆C blend films with 0.2 vol% DIO are 80, 82 and 83 nm, respectively.

Table S10. Hole and electron mobilities for FTAZ:acceptor blend films.

FTAZ:acceptor	μ_h [cm ² V ⁻¹ s ⁻¹]	μ_e [cm ² V ⁻¹ s ⁻¹]	μ_h/μ_e
FTAZ:CO ₆ IC	7.32×10 ⁻⁵	6.60×10 ⁻⁶	11.09
FTAZ:CO ₆ FIC	1.45×10 ⁻⁴	2.07×10 ⁻⁵	7.00
FTAZ:CO ₆ DFIC	1.23×10 ⁻⁴	1.29×10 ⁻⁵	9.53

9. AFM

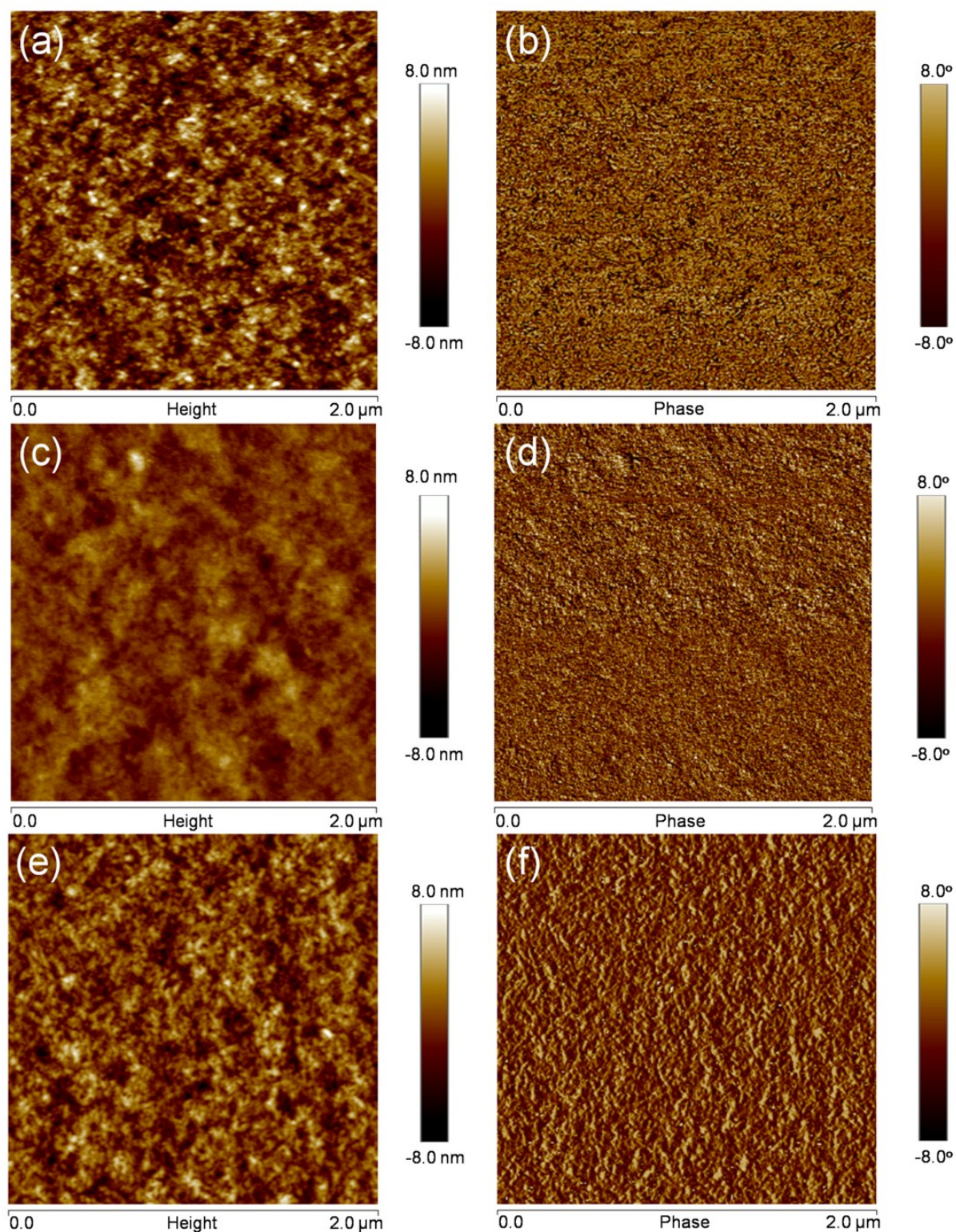


Fig. S19 AFM height (left) and phase (right) images for the blend films. (a) and (b), FTAZ:CO₆IC film with 0.2 vol% DIO; (c) and (d), FTAZ:CO₆FIC film with 0.2 vol% DIO; (e) and (f), FTAZ:CO₆DFIC film with 0.2 vol% DIO.

References

- [1] Z. Xiao, X. Jia, D. Li, S. Wang, F. Liu, J. Chen, S. Yang, T. P. Russell and L. Ding, *Sci. Bull.* 2017, **62**, 1494.
- [2] D. He, L. Qian and L. Ding, *Polym. Chem.*, 2016, **7**, 2329.
- [3] S. C. Price, A. C. Stuart, L. Yang, H. Zhou and W. You, *J. Am. Chem. Soc.*, 2011, **133**, 4526.
- [4] Y. Sun, J. H. Seo, C. J. Takacs, J. Seifter and A. J. Heeger, *Adv. Mater.*, 2011, **23**, 1679.
- [5] C. Duan, W. Cai, B. Hsu, C. Zhong, K. Zhang, C. Liu, Z. Hu, F. Huang, G. C. Bazan, A. J. Heeger and Y. Cao, *Energy Environ. Sci.*, 2013, **6**, 3022.